Deakin Research Online

This is the published version:

Atwell, Dale and Barnett, Matthew 2007-12-12, Extrusion limits of magnesium alloys, *Metallurgical and Materials Transactions A-Physical Metallurgy and Materials Science*, vol. 38, no. 12, pp. 3032-3041.

Available from Deakin Research Online:

http://hdl.handle.net/10536/DRO/DU:30007596

Copyright : 2007 ASM International. This paper was published in *Metallurgical and Materials Transactions A-Physical Metallurgy and Materials Science*, vol. 38, no. 12, pp. 3032-304 and is made available as an electronic reprint with the permission of ASM International.

One print or electronic copy may be made for personal use only. Systematic or multiple reproduction, distribution to multiple locations via electronic or other means, duplications of any material in this paper for a fee or for commercial purposes, or modification of the content of this paper are prohibited.

Extrusion Limits of Magnesium Alloys

DALE L. ATWELL and MATTHEW R. BARNETT

Magnesium alloys are generally found to be slower to extrude than aluminum alloys; however, limited quantitative comparisons of the actual operating windows have been published. In this work, the extrusion limits are determined for a series of commercial magnesium alloys (M1, ZM21, AZ31, AZ61, and ZK60). These are compared with the limits established for aluminum alloy AA6063. The maximum extrusion speed of alloy M1 is shown to be similar to AA6063. Alloys ZM21, AZ31, ZK60, and AZ61 exhibit maximum extrusion speeds 44, 18, 4, and 3 pct, respectively, of the maximum measured for AA6063. For AZ31, the maximum extrusion speed is increased by 22 pct after homogenization and by 64 pct for repeat extrusions. The variation in the extrusion limits with changing alloy content is rationalized in terms of differences in the hot working flow stress and solidus temperature.

DOI: 10.1007/s11661-007-9323-2
© The Minerals, Metals & Materials Society and ASM International 2007

I. INTRODUCTION

IT is reported that magnesium alloys are generally $^1/_3$ to $^2/_3$ slower to extrude than aluminum alloys.[1] This makes a significant contribution to the cost of production. Both hydrostatic[2–6] and indirect[4,6,7] extrusion methods have been employed to permit magnesium alloys to be extruded at higher rates. Nevertheless, direct extrusion is very common, and improved knowledge of the performance of magnesium in this process is expected to lead to alloys with enhanced extrudability.[8]

An effective means of assessing relative extrusion rates is the extrusion limit diagram. These have been used to describe the extrusion performance of a number of aluminum alloys,[9–14] but the approach appears to have been applied to magnesium alloys only in a few cases.[15–18] Despite the infrequent use of the full limit diagram, the degree to which the maximum extrusion speed of the Mg-Al-Zn alloy series is raised by lowering the aluminum or zinc level has been quantified in a number of cases.[16,18–20] As expected, lowering these alloying additions also comes at a cost to the mechanical performance of the product.[4] In contrast to this, it has been shown that manganese additions improve mechanical properties without significantly lowering the extrusion speed.[18,20] Furthermore, in the Mg-Zn-Zr alloy series, the addition of zirconium actually increases the extrudability by raising the solidus temperature.[21] There are also a limited number of cases where the extrusion performance has been compared for isolated alloys.[2,3,5,22–25] Systematic comparison over a range of alloys does not appear to have been carried out.

The present work aims to quantify the extrusion speed limits for key wrought magnesium alloys using a laboratory scale extrusion press in a manner that allows the effects of the different alloying additions to be assessed. A common fast extruding 6XXX series aluminum alloy is also examined for comparison.

DALE L. ATWELL, Research Engineer, and MATTHEW R. BARNETT, QEII Research Fellow, are with the Cooperative Research Centre for Cast Metals Manufacturing (CAST), Geelong Technology Precinct, Deakin University, Geelong, VIC 3217, Australia. Contact e-mail: datwell@deakin.edu.au

Manuscript submitted December 18, 2006.
Article published online October 12, 2007

II. EXPERIMENTAL METHOD

The billets used in this investigation measured Ø30 mm × 20 mm and were of the commercial magnesium alloy grades M1, ZM21, AZ31, AZ61, and ZK60, and the aluminum alloy AA6063. The chemical composition of the magnesium billets is shown in Table I. The M1, ZM21, AZ31, and AZ61 alloy billets were acquired in the extruded (wrought) condition. These should be thought of as being in a homogenized state. This condition can also be considered to replicate the first stage of a two-stage extrusion process, which is not uncommon for many magnesium alloys.[7] The AA6063, ZK60 alloys and an additional sample of the AZ31 alloy were acquired as billets in the cast condition.

The cast AA6063 billets were given a standard[26] homogenization heat treatment by soaking at 580 °C for 6 hours followed by step cooling at 275 °C for 2 hours. The cast ZK60 and cast AZ31 billets were given homogenization heat treatments at 430 °C for 8 hours and 400 °C for 48 hours respectively in a protective argon atmosphere. Following homogenization, all billets were removed from the furnace and cooled to room temperature in still air. AZ31 billets were each extruded in the as-cast, homogenized, and wrought states in order to illustrate the impact of billet preparation on the extrusion limits.

The M1 billet contained a bimodal microstructure with very large elongated grains (up to 1 mm in length) that were surrounded by necklaces of finer grains (Figure 1). The wrought alloys ZM21, AZ31, and AZ61 displayed a homogenous microstructure with equiaxed grains of 47, 23, and 15 μm, respectively (average linear intercept length). The cast AZ31 and ZK60 billets displayed average linear intercept lengths

Table I. Compositions of the Magnesium Alloys Tested (Weight Percent)

Alloy	Mg	Al	Zn	Mn	Zr
M1	~bal	—	0.02	1.62	—
ZM21	~bal	0.01	2.2	0.8	—
AZ31 (cast)	~bal	2.87	0.83	0.45	—
AZ31 (wrought)	~bal	2.83	0.86	0.73	—
AZ61	~bal	6.0	0.99	0.26	—
ZK60	~bal	—	5.40	0.01	0.59

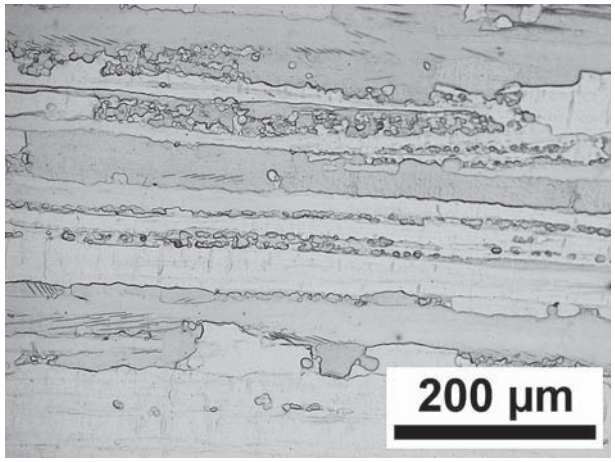

Fig. 1—Microstructure of the M1 billet.

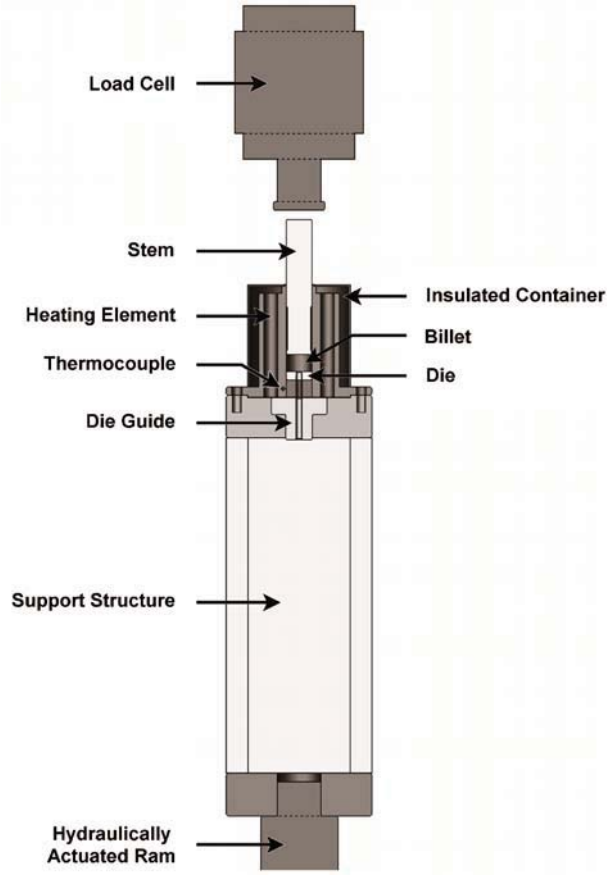

Fig. 2—Sectioned schematic representation of the extrusion rig.

of 316 and 87 μm, respectively. Homogenization provided a detectable reduction in the population of intermetallic particles but no obvious change in the grain size.

Direct extrusion was performed using the laboratory rig shown schematically in Figure 2. The rig was housed in a servo-hydraulic testing frame with a 350 kN load capacity providing a maximum ram pressure limit of 512 MPa.

The billet, die, and container were heated *in situ* using electric heating elements and the billets were allowed to soak at the test temperature for 5 minutes prior to extrusion. The temperature was measured in the container using a thermocouple. A calibration curve was employed to establish the billet temperature from knowledge of the container thermocouple temperature. The billet surface was coated with a molybdenum disulfide based dry solid film lubricant to assist ejection of the discard. A 0.25-mm radial clearance between the stem and the container wall meant that the billet surface was retained as a skin with the discard after extrusion.

The profile extruded was a solid Ø5.4-mm round rod (which gives an extrusion ratio of 30) using a flat faced die with a 90 deg entry angle and 1 mm parallel die land. The initial billet temperature and ram speed were varied to determine their effects on the extrusion pressure and the extruded surface. The measured ram displacement was adjusted to account for the elasticity of the rig.

The extrusion temperatures employed ranged from 250 °C to 620 °C at ram speeds up to 40 mms^{-1}. This enabled near industrial extrusion speeds to be considered. Ram speeds slower than 1 mms^{-1} were not employed, because they were considered to be industrially irrelevant.

III. RESULTS

A. *Extrusion Pressure*

Examples of typical extrusion ram pressure and speed traces are shown in Figure 3 for homogenized AZ31 and AA6063 billet. These traces are typical of aluminum and magnesium alloys undergoing direct extrusion. Of note is the higher peak for magnesium compared to aluminum despite similar pressures at higher displacements. The speed trace attains the set value after a short transient. The attainment of the desired speed often coincided with the peak in the pressure curve.

To describe the variation in the peak pressure, P, with extrusion conditions, the Zener–Holloman parameter, Z, was evaluated according to

$$Z = \dot{\varepsilon} \exp\left(\frac{Q}{8.314T}\right) \quad [1]$$

where the strain rate, $\dot{\varepsilon}$, is given by[16]

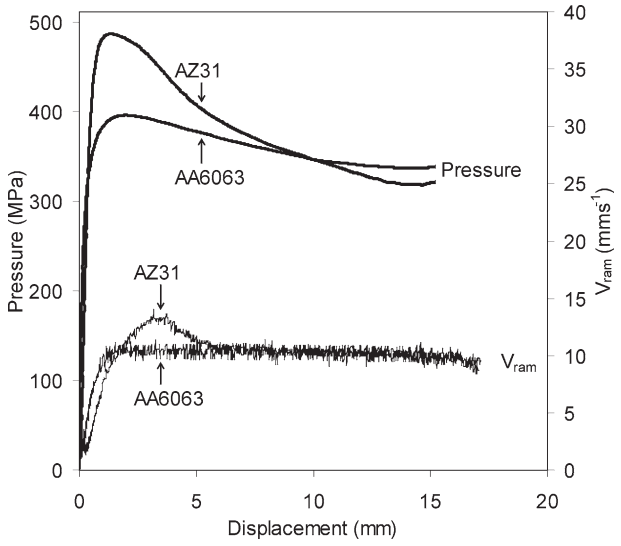

Fig. 3—Typical pressure-displacement trace with corresponding ram speed for homogenized AZ31 and AA6063 billet at an initial billet temperature of 375 °C.

$$\dot{\varepsilon} \approx \frac{9.6R^{0.6}V_R}{D_B} \qquad [2]$$

where T is the billet temperature (not corrected for deformation heating), Q is the apparent activation energy for deformation (the activation energy for self-diffusion in magnesium of 135 kJ/mol[27,28] was used for the magnesium alloys and 141.55 kJ/mol[9] was used for AA6063), R is the extrusion ratio, V_R is the ram speed, and D_B is the billet diameter.

The reader should note that Q is expected to actually vary with temperature and alloy content.[29] A standard value of Q was chosen to permit the influence of the deformation conditions and the alloy content on peak pressure to be plotted on a single plot. This assumption introduces an error that is negligible given that this approach also ignores the effect of deformation heating.

Despite these simplifying steps, the peak pressure scales quite well with the values of Z obtained (Figure 4(a)). The relationship is best described with a logarithmic law:

$$P = c_1 Ln(Z) + c_2 \qquad [3]$$

where c_1 and c_2 are empirical constants.

The influence of alloy composition on extrusion pressure is captured in Figure 4(b), which shows the trend lines obtained from plots similar to Figure 4(a). It is apparent that the influence of the deformation conditions on the peak pressure is, in general, consistent across all the magnesium alloys. The intensity of the effect of Z is, however, stronger in the magnesium alloys than in the aluminum alloy (AA6063). The values of Q used here for the two metals are sufficiently similar for this phenomenon to be taken as a real effect. Thus, it is evident that magnesium alloys display an increased sensitivity of the extrusion pressure to speed and temperature than for aluminum alloy AA6063. It is also clear that the magnitude of the peak pressure varies with alloy content. Generally, the leaner magnesium alloys generate lower peak pressures. For most of the conditions examined, the magnesium alloys displayed a higher peak pressure than the aluminum alloy (AA6063).

B. *Extruded Surfaces*

The surface condition of the extrusions was examined visually to determine the limiting speed for crack initiation. Examples of the surfaces generated from the homogenized AZ31 billet are presented in Figure 5.

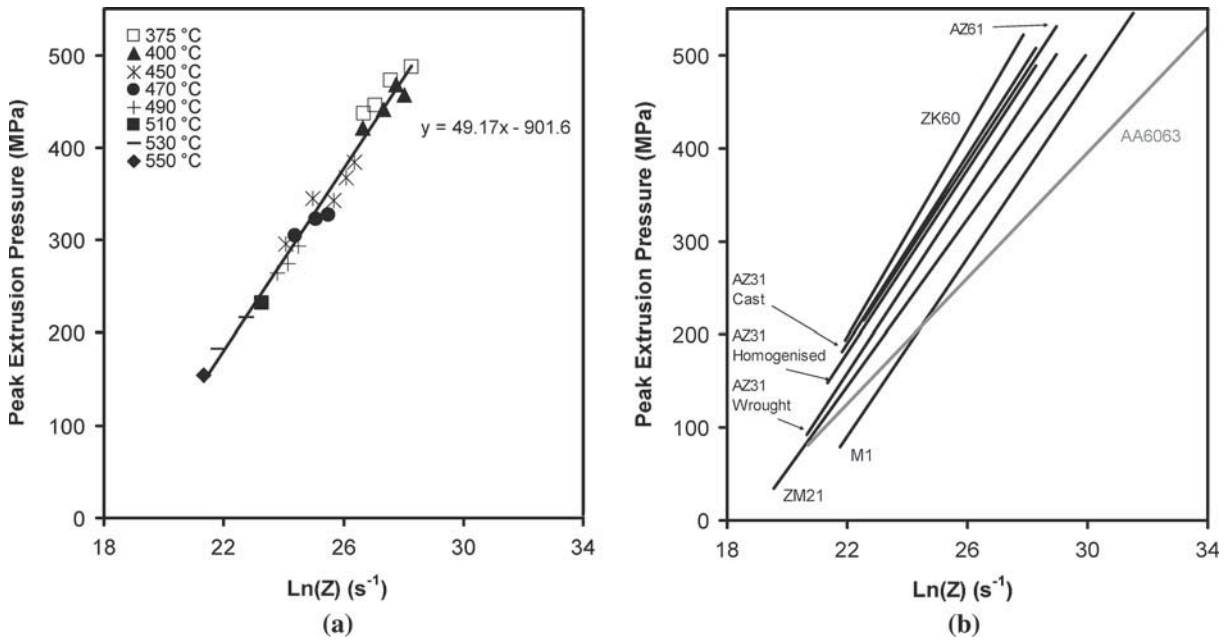

Fig. 4—Influence of the Zener–Holloman parameter on the peak pressure: (*a*) AZ31 (homogenized) and (*b*) summary of trends.

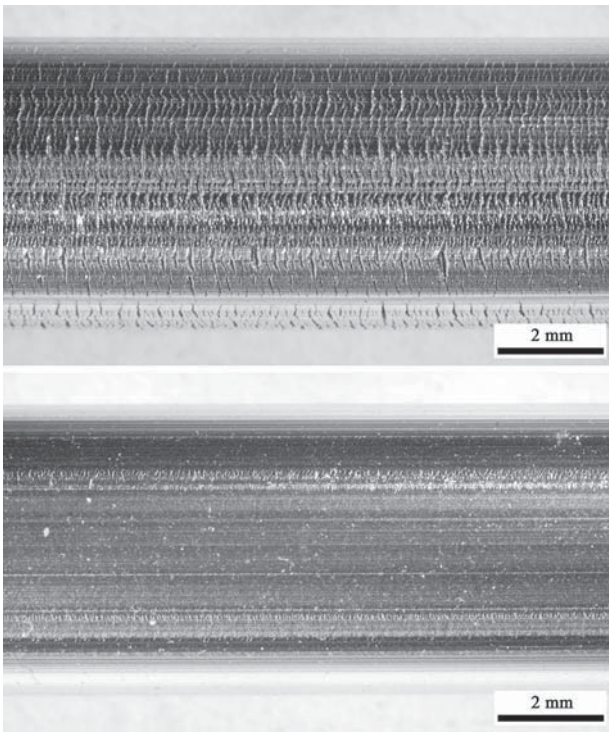

Fig. 5—Examples of the surfaces obtained in the present work for homogenized AZ31 billet extruded at 490 °C, at V_R 10 mms^{-1} (top) and 7 mms^{-1} (bottom).

With increasing speed or temperature, a condition was eventually reached where surface cracking was observed. This is consistent with the phenomenon of hot shortness.[9]

All the extruded surfaces showed the presence of minor die lines, which appear exaggerated in the high-magnification images shown in Figure 5. Investigation of the contributing factors to their occurrence (for instance, die design, die wear, surface coatings, and material pickup) was beyond the scope of this work. However, the reader should note that die lines (caused by pickup) rather than cracking often dictate the high-temperature extrusion limit of aluminum alloys.[9]

For the M1 billet, an irregular roughening of the surface was observed as the billet temperature was increased (Figure 6). This is similar in appearance to the "orange peel" defect seen in sheet forming and always occurred prior to cracking. A similar rough surface was also encountered during extrusion at low billet temperatures and speeds. None of the other alloys displayed this behavior.

An additional cosmetic defect observed during high-temperature extrusion of the M1 and ZM21 alloys was the formation of a black oxide on the extruded surface. This defect was only observed in isolated samples extruded just below the cracking limit temperature.

C. *Extrusion Limit Diagrams*

The pressure and surface quality data are plotted as extrusion limits in Figure 7. These figures show the limiting pressure for the lab press and the onset of cracking in terms of the initial billet temperature and the extrusion exit speed. Each limit diagram encompasses multiple individual extrusions spanning a range of conditions.

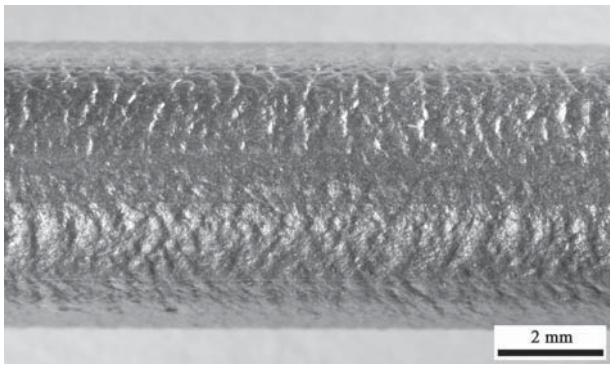

Fig. 6—An example of the surface obtained in the present work for M1 billet showing the orange peel defect (extruded at V_R 15 mms^{-1} at 582 °C).

The surface condition was inspected and categorized into one of four conditions. The open symbols shown indicate a successful extrusion without the presence of surface cracks. This category is further divided into "acceptable" (open circles), indicating visually smooth and bright surfaces though some die lines may be present, and "cosmetic damage" (open triangles), indicating either defect "orange peel," "blackening," or "low speed roughening." The shaded symbols represent conditions where cracking initiated part way along the length of the extrusion. The filled symbols indicate severe cracking along the entire length. A locus was drawn between the regions exhibiting cracking and no cracking.

Extrusion conditions that generated a ram pressure exceeding the 512 MPa capacity limit of the press are indicated by the star symbols. The position of the pressure limit locus was determined using semiempirical equations. Combining Eqs. [1] through [3] with the relationship between the ram speed, V_R, and the extrusion speed, V_E ($V_E = RV_R$), yields

$$P = c_1 \ln\left[\left(\frac{9.6V_E}{D_B R^{0.4}}\right)\exp\left(\frac{Q}{8.314T}\right)\right] + c_2 \qquad [4]$$

which, on rearranging to make V_E the subject, yields

$$V_E = \frac{D_B R^{0.4}}{9.6}\exp\left(\frac{P - c_2}{c_1} - \frac{Q}{8.314T}\right) \qquad [5]$$

where V_E, D_B, P, Q, and T have the units ms^{-1}, m, MPa, J/mol, and degrees K, respectively.

The cosmetic orange peel defects observed with the M1 alloy mean that the extrusion window is significantly smaller when surface finish is critical (Figure 7(b)). This defect gradually increases in severity. As a consequence, the corresponding limit is not as well defined as the cracking limit.

The extrusion limits presented in Figures 7(d) through (f) represent AZ31 billet with different initial pretreatments and are compared in Figure 8. The broadest

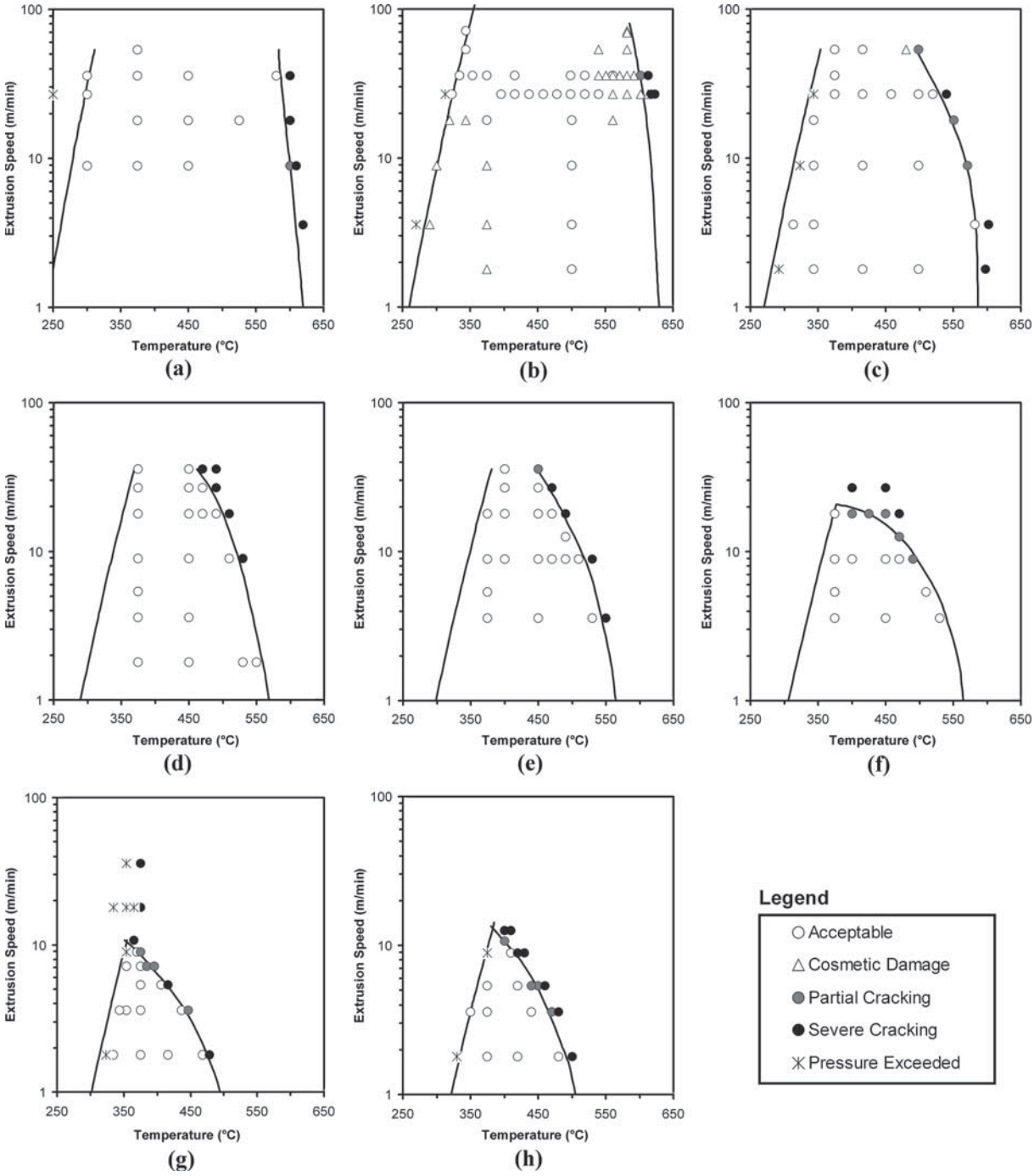

Fig. 7—Extrusion limit diagrams for the present study. The left (pressure) limit was determined using empirical model extrapolation. The right (cracking) limit is a curve fitted through the partial cracking data: (*a*) homogenized AA6063, (*b*) wrought M1, (*c*) wrought ZM21, (*d*) wrought AZ31, (*e*) homogenized AZ31, (*f*) as-cast AZ31, (*g*) wrought AZ61, and (*h*) homogenized ZK60.

window corresponds to the wrought billet, with the narrowest window the unhomogenized as-cast billet. There is a significant difference in the cracking limit for the different conditions at intermediate billet temperatures. This difference is not apparent at high temperatures, where all the samples display a similar limit. A possible explanation for this is that at high billet temperatures, the time spent (5 min) soaking *in situ* is sufficient to provide a degree of homogenization or solid solution prior to extrusion. It is pertinent to note that the limit window for the as-cast and homogenized material is quite similar to that of the wrought sample.

A comparison of the extrusion limits for the different alloys is provided in Figure 9. These limits relate to the extrusion of wrought billets with the exception of ZK60 and AA6063, which represent billets that have been cast and homogenized. For some alloys, the limits are

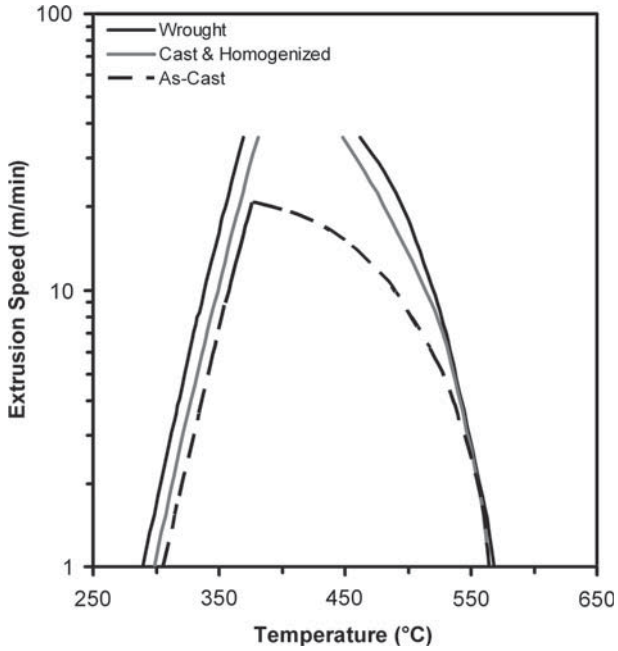

Fig. 8—Effect of billet condition on the extrusion limits of AZ31 (pressure limit: 512 MPa).

incomplete due to the speed limitations of the press. By reducing the pressure limit value in Eq. [5] from 512 MPa (Figure 9(a)) to 190 MPa (Figure 9(b)), smaller operating windows are obtained. (Note that in each case the cracking limit is unchanged.) This change permits comparison of the maximum extrusion speeds.

For the 512 MPa ram pressure limit, the extrusion windows of all the magnesium billets are smaller than the aluminum grade. However, in Figure 9(b), the extrusion window for the aluminum alloy falls within that for M1. This can be understood in terms of the reduced sensitivity of AA6063 to temperature and extrusion speed (Figure 4(b)).

The maximum extrusion speeds vary from 1.4 to 100 m/min in Figure 9(b), but it should be remembered that these values are specific to the present geometry and assumed press limits. Nevertheless, the relative extrusion rates for the different alloys are expected to be of general applicability. Inspection of Figure 9(b) reveals that the relative maximum extrusion speed in alloy M1 is ~2.5 times faster than AA6063 if cracking is considered the limiting factor. However, consideration of the cosmetic limits brings the maximum extrusion speed of M1 in line with that predicted for AA6063. Alloys ZM21 and AZ31 show maximum extrusion speeds 44 and 18 pct, respectively, of that seen for AA6063. Alloys AZ61 and ZK60 display maximum extrusion speeds 4 and 3 pct of that seen in AA6063. These more heavily alloyed magnesium alloys show quite low maximum extrusion speeds.

It is interesting to note that the present data suggest that the slow extrusion speeds of magnesium alloys should be attributed to the nature of the particular alloying additions employed rather than to an inherent property of the metal. Alloy M1 extrudes here at a rate comparable to AA6063, which is generally considered to be a "fast" extruding aluminum alloy.

IV. DISCUSSION

A. *Comparison with Other Workers*

The present cracking limits agree quite well with other published limits for wrought[8] and as-cast[16,18,19] AZ31 billet (Figures 10 and 11). Of note is the marked improvement in the correlation of the present limits

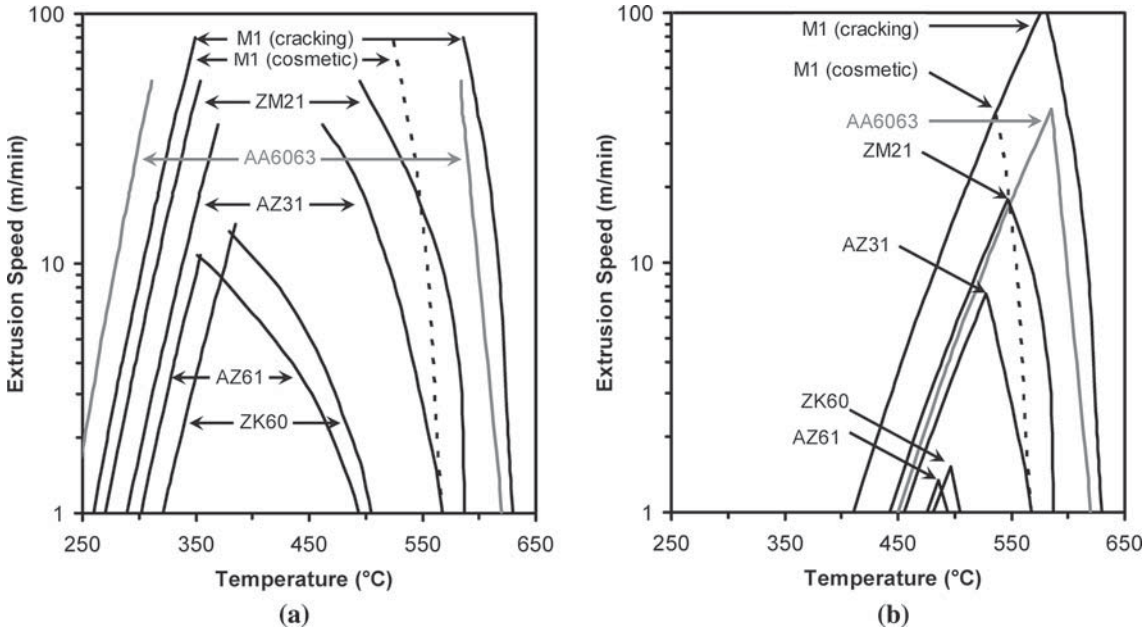

Fig. 9—Collated extrusion limit diagrams: (*a*) 512 MPa pressure limit and (*b*) 190 MPa pressure limit.

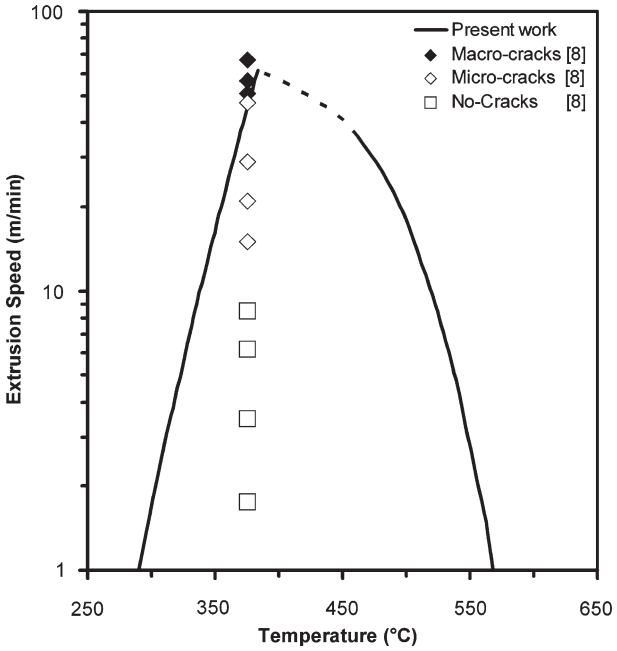

Fig. 10—Wrought AZ31 billet extrusion limits compared with the cracking limit identified by Sillekens.[8]

with the published experimental data shown in Figure 11. This result highlights the inexact nature of the earlier empirically modeled limits for AZ31.[16]

The present work may also be compared with the limits of other magnesium alloys reported by Lass *et al.*[25] Although limited information is provided about the extrusion conditions in that study, a relative comparison may be made by normalizing both data sets to the maximum extrusion rate obtained for AZ31

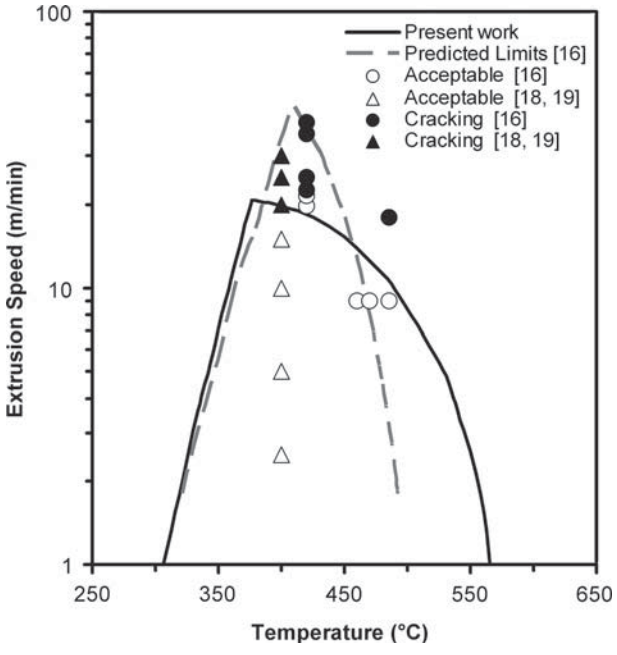

Fig. 11—As-cast AZ31 billet extrusion limits compared with the cracking limits identified by Barnett *et al.*[16] and Murai *et al.*[18,19]

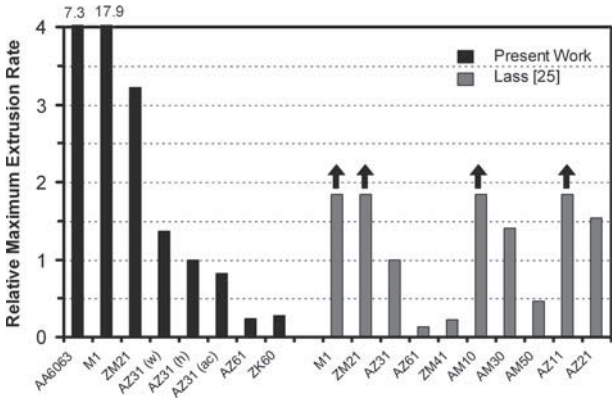

Fig. 12—Maximum extrusion speed of present and published alloys relative to homogenized AZ31 magnesium billet (AZ31 alloy = 1).

(Figure 12). The arrows shown in the figure indicate that the maximum extrusion rate was unable to be determined due to press limitations. Despite this, the general trends in the reported maximum speeds are consistent with the present work.

B. *Modeling the Limits*

To assist in understanding the extrusion behavior of the present alloys, semiempirical expressions are developed in Sections 1 and 2 below to describe the pressure limit (using the hot working flow stress) and the cracking limit (using the solidus temperature).

1. *Pressure*

The peak extrusion pressure, P, can be considered a function of the material flow stress, σ, and the extrusion parameters (extrusion ratio, friction conditions, die complexity, and the length and diameter of the billet).[9] As the extrusion parameter terms remain constant in the present work, they may be grouped into a single constant, k_1, so the pressure can be approximated by

$$P = k_1\sigma \qquad [6]$$

The material flow stress of magnesium alloys can be estimated from the deformation conditions by assuming a power-law dependence on the Zener–Holloman parameter.[30]

$$\sigma = k_2 Z^m = \frac{\sigma_{\text{ref}}}{Z_{\text{ref}}^m} Z^m \qquad [7]$$

where k_2 is a constant, m is the strain rate sensitivity, and σ_{ref} is a reference flow stress corresponding to a reference Z condition, Z_{ref}. The reader should note that a hyperbolic sine law dependence of the stress on Z is generally employed for aluminum alloys, because it describes both the low and high stress behaviors. However, for the present extrusion conditions, the stresses encountered are expected to be in the low stress region,[16] where the hyperbolic sine law simplifies to a power law. Combining Eqs. [6] and [7] with Eqs. [1] and [2] and rearranging gives

$$P = k_1 \frac{\sigma_{\text{ref}}}{Z_{\text{ref}}^m} \frac{9.6^m V_E^m}{D_B^m R^{0.4m}} \exp\left(\frac{mQ}{8.314T}\right) \quad [8]$$

where V_E is the velocity of the extrusion exiting the die. Grouping the terms constant in the present work into a single constant, k, yields

$$P = k\sigma_{\text{ref}} V_E^m \exp\left(\frac{mQ}{8.314T}\right) \quad [9]$$

2. *Size of Operating Window*

For the present purposes, we seek an expression for the "width" (in degrees K) of the extrusion window at some reference extrusion speed. (A speed of 1 m/min is employed here because this value is sufficiently low to avoid the complication of overly high levels of deformation heating.) This width, ΔT^*, is the difference between the temperature, T_P, of the pressure limit and the temperature, T_C, of the cracking limit, at this speed.

The temperature, T_P, corresponding to the pressure limit, P_{lim} (at the reference speed), can be obtained by rearranging Eq. [9] and substituting unity for V_E:

$$T_P = \frac{mQ}{8.314 \ln\left(P_{\text{lim}}/k\sigma_{\text{ref}}\right)} \quad [10]$$

To apply this expression, it is necessary to determine values for σ_{ref}. This was performed here using uniaxial compression at a temperature of 350 °C and a constant strain rate of 1 s^{-1}. The flow curves thus obtained are illustrated in Figure 13. (The flow behavior of homogenized AZ31 is of note as its steady state stress is higher than that obtained for the wrought AZ61 despite its lower aluminum content. This may be attributable to the influence of intermetallic particles in the homogenized AZ31 material.) Values for σ_{ref} were read off this plot for values corresponding to a strain of unity. These values provide an approximation for the steady-state stress, which is expected to be most relevant for the extrusion pressure.

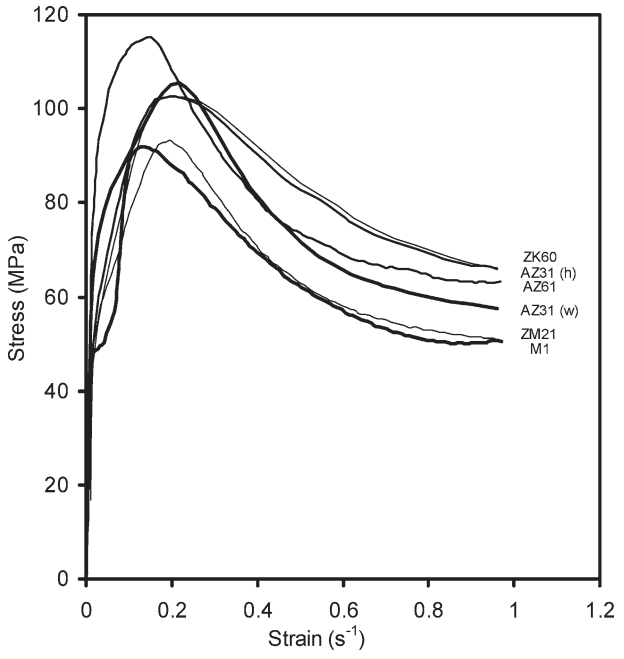

Fig. 13—Flow curves from uniaxially compressed billet material at 350 °C, 1 s^{-1} (AZ31 data taken from[31]).

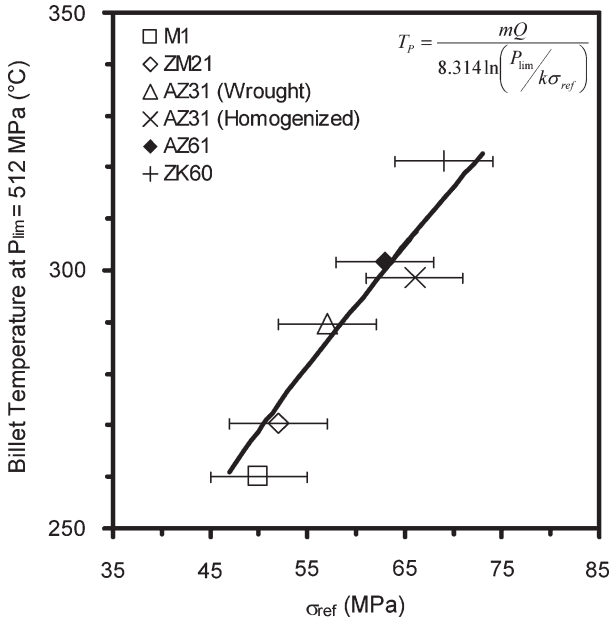

Fig. 14—The billet temperature at the 512 MPa pressure limit *vs* σ_{ref}. In this case $k = 0.154$. (Error bars are estimates of the range based on repeat tests.)

In Figure 14, Eq. [10] is fitted by adjusting k to the values of T_P obtained from Figure 9(a) for extrusion speeds of 1 m/min. An m value of 0.14 was assumed for all the magnesium alloys.[30] It can be seen that Eq. [10] provides a reasonable description of the data.

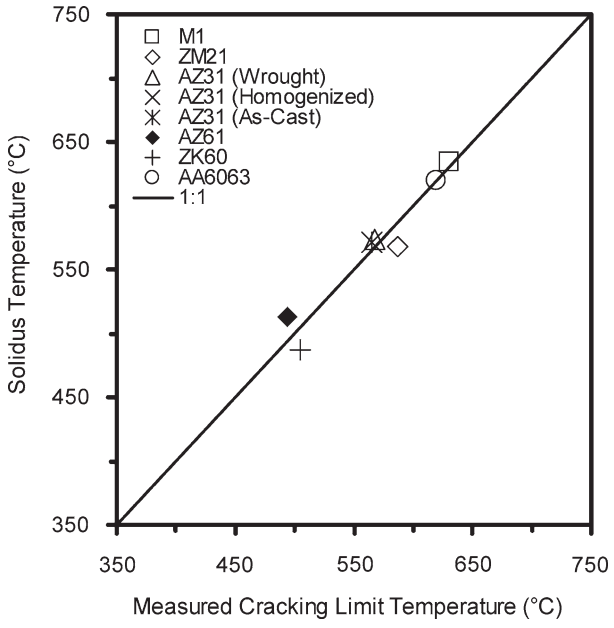

Fig. 15—Solidus temperature *vs* the cracking limit temperature at a V_E of 1 m/min.

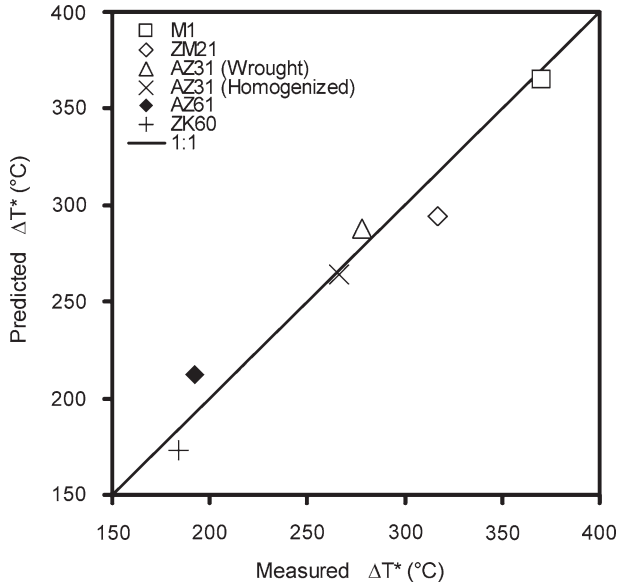

Fig. 16—The ΔT^* predicted from Eq. [11] *vs* the ΔT^* measured from the extrusion limit diagrams.

In making this comparison, it is important to be aware of the differences in deformation modes between compression and extrusion. The stresses measured from the compression test are of a similar magnitude to those expected to be encountered during extrusion,[16] but differences are expected due to differences in crystallographic texture and strain severity. Nevertheless, it can be concluded that the relative pressure limits obtained in the present extrusion experiments can be rationalized fairly simply in terms of the relative hot working flow stresses.

The temperature, T_C, corresponding to the cracking limit should fall close to the solidus temperature.[9] Accordingly, the solidus temperature, T_{sol} (ascertained using THERMOCALC), is compared in Figure 15 with the cracking limit temperature obtained in Figure 9(a) for an extrusion rate of 1 m/min. The agreement between the two values is good within the experimental error. The solidus temperature thus provides a reasonable first-order estimate for the nominal billet temperature at which cracking can be expected for the present slow extrusion speed. In the case of faster extrusion speeds, an increasing deviation between the two values is expected due to the effect of deformation heating.

The width of the extrusion window, ΔT^*, at the extrusion rate of 1 m/min, can thus be given by

$$\Delta T^* = T_{\text{sol}} - \frac{mQ}{8.314 \ln \left(P_{\text{lim}} / k\sigma_{\text{ref}} \right)} \qquad [11]$$

Figure 16 compares the predicted with the experimental values for ΔT^*. It is clear that the width of the extrusion limit windows of the present magnesium alloys can be estimated using Eq. [11], once values for k, the reference flow stress and the solidus temperature are known. The wider the extrusion limit window, the greater the maximum extrusion speed.

V. CONCLUSIONS

1. The extrudability of magnesium alloys improves relative to aluminum (AA6063) with reducing Z values (*i.e.*, higher billet temperatures or slower rates) due to a stronger influence of Z on the peak extrusion pressure.
2. Extruding homogenized AZ31 billet rather than as-cast billet resulted in a 22 pct increase in the maximum extrusion speed. Similarly, processing pre-extruded (wrought) AZ31 billet produced a 64 pct increase in the maximum extrusion speed over as-cast billet.
3. Although the M1 alloy exhibited the largest extrusion window of the magnesium alloys, the occurrence of the orange peel surface defect prior to cracking reduces its relative extrudability if this defect is to be avoided.
4. Alloying magnesium with aluminum or zinc lowers the maximum extrusion speed.
5. The width of the extrusion window can be estimated quite simply once the solidus temperature and the flow stress at a reference hot working condition are known.

ACKNOWLEDGMENTS

The assistance of John Vella with the development of the extrusion rig and Chris Davies for calculating the solidus temperatures using THERMOCALC is gratefully acknowledged. Deakin University is a core participant in the CRC for Cast Metals Manufacturing (CAST), which was established under and is supported in part by the Australian Government's Cooperative Research Centre scheme.

REFERENCES

1. F.E. Katrak, J.C. Agarwal, F.C. Brown, M. Loreth, and D.L. Chin: *Magnesium Technology*, Nashville, TN, Mar. 12–16, 2000, H.I. Kaplan, J.N. Hryn, and B.B. Clow, eds., TMS, Warrendale, Pennsylvania, pp. 351–54.
2. K. Savage and J.K. King: *DGM Conf. Magnesium Alloys and Their Applications*, Munich, Sept. 26–28, 2000, K.U. Kainer, ed., Wiley-VCH, Weinheim, Germany, pp. 609–14.
3. W.H. Sillekens, J.A.F.M. Schade van Westrum, A.J. den Bakker, and P.-J. Vet: *Processing & Manufacturing of Advanced Materials*, Leganés, Madrid, July 7–11, 2003, T. Chandra, J.M. Torralba, and T. Sakai, eds., Trans Tech Publications, Uetikon-Zurich, Switzerland, pp. 629–36.
4. J. Swiostek, J. Bohlen, D. Letzig, and K.U. Kainer: *6th DGM Conf. "Magnesium Alloys and Their Applications,"* Weinheim, Germany, 2004, K.U. Kainer, ed., Wiley-VCH, Weinheim, Germany, pp. 278–84.
5. J. Bohlen, J. Swiostek, W.H. Sillekens, P.-J. Vet, D. Letzig, and K.U. Kainer: *Magnesium Technology*, San Francisco, CA, Feb. 13–17, 2005, N.R. Neelameggham, H.I. Kaplan, and B.R. Powell, eds., TMS, Warrendale, Pennsylvania, pp. 241–46.
6. J. Swiostek, J. Bohlen, D. Letzig, and K.U. Kainer: *Magnesium—Science, Technology and Applications*, Beijing, Sept. 20–24, 2004, Y.-W. Mai, G.E. Murch, and F.H. Wohlbier, eds., Trans Tech Publications, Uetikon-Zurich, Switzerland, pp. 491–94.
7. K.B. Mueller: *Magnesium Technology*, Seattle, WA, Feb. 17–21, 2002, H.I. Kaplan, ed., TMS, Warrendale, Pennsylvania, pp. 187–92.

8. W. H. Sillekens: *Light Metals Technology*, St. Wolfgang, Austria, June 8–10, 2005, H. Kaufmann, ed., LKR, Ranshofen, Austria, pp. 137–42.
9. T. Sheppard: *Extrusion of Aluminium Alloys*, Kluwer Academic Publishers, Dordrecht, 1999, p. 420.
10. M.G. Tutcher and T. Sheppard: *Met. Technol.*, 1980, vol. 7 (12), pp. 488–93.
11. B.J. Meadows and M.J. Cutler: *J. Inst. Met.*, 1969, vol. 97, pp. 321–26.
12. T. Sheppard, P.J. Tunnicliffe, and S.J. Patterson: *J. Mech. Working Technol.*, 1982, vol. 6 (4), pp. 313–31.
13. T. Sheppard: *Mater. Sci. Technol.*, 1993, vol. 9, pp. 430–40.
14. M.P. Clode and T. Sheppard: *Mater. Sci. Technol.*, 1993, vol. 9, pp. 313–18.
15. M.R. Barnett, D. Atwell, C. Davies, and R. Schmidt: *Light Metals Technology*, St. Wolfgang, Austria, June 8–10, 2005, H. Kaufmann, ed., LKR, Ranshofen, Austria, pp. 161–66.
16. M.R. Barnett, J.-Y. Yao, and C. Davies: *Light Metals Technology*, Brisbane, Australia, Sept. 18–20, 2003, A.K. Dahle, ed., CAST, Brisbane, Australia, pp. 333–38.
17. R.Y. Lapovok, M.R. Barnett, and C.H.J. Davies: *J. Mater. Process. Technol.*, 2004, vol. 146 (3), pp. 408–14.
18. T. Murai, S.-I. Matsuoka, S. Miyamoto, and Y. Oki: *Mater. Sci. Forum.*, 2003, vol. 419–22, pp. 349–54.
19. T. Murai, S.-I. Matsuoka, S. Miyamoto, Y. Oki, S. Nagao, and H. Sano: *J. Jpn. Inst. Light Met.*, 2003, vol. 53 (1), pp. 27–31.
20. T. Murai, H. Oguri, and S.-I. Matsuoka: *Magnesium—Science, Technology and Applications*, Beijing, China, Sept. 20–24, 2004, Y.-W. Mai, G.E. Murch, and F.H. Wohlbier, eds., Trans Tech Publications, Uetikon-Zurich, Switzerland, pp. 515–18.
21. J.P. Doan and G. Ansel: *AIME*, 1947, vol. 171, pp. 286–305.
22. W.H. Sillekens and J. Bohlen: *6th DGM Conf. "Magnesium Alloys and their Applications,"* Weinheim, Germany, 2004, K.U. Kainer, ed., Wiley-VCH, Weinheim, Germany, pp. 1046–51.
23. A.J.D. Bakker, W.H. Sillekens, J. Bohlen, K.U. Kainer, and G. Barton: *6th DGM Conf. "Magnesium Alloys and their Applications,"* Weinheim, Germany, 2004, K.U. Kainer, ed., Wiley-VCH, Weinheim, Germany, pp. 324–30.
24. C. Jaschik (Sp), H. Haferkamp, and M. Niemeyer: *DGM Conf. "Magnesium Alloys and Their Applications,"* Munich, Sept. 26–28, 2000, K.U. Kainer, ed., Wiley-VCH, Weinheim, Germany, pp. 41–46.
25. J.-F. Lass, F.-W. Bach, and M. Schaper: *Magnesium Technology*, San Francisco, CA, Feb. 13–17, 2005, N.R. Neelameggham, H.I. Kaplan, and B.R. Powell, eds., TMS, Warrendale, Pennsylvania, pp. 159–64.
26. Y. Birol: *J. Mater. Process. Technol.*, 2004, vol. 148 (2), pp. 250–58.
27. S.S. Vagarali and T.G. Langdon: *Acta Metall.*, 1981, vol. 29 (12), pp. 1969–82.
28. P.G. Shewmon and F.N. Rhines: *J. Met. (AIME)*, 1954, vol. 200, pp. 1021–25.
29. A. Galiyev, R. Kaibyshev, and G. Gottstein: *Acta Mater.*, 2001, vol. 49 (7), pp. 1199–1207.
30. A.G. Beer and M.R. Barnett: *Magnesium Technology*, Seattle, WA, Feb. 17–21, 2002, H.I. Kaplan, ed., TMS, Warrendale, Pennsylvania, pp. 193–98.
31. A.G. Beer: Ph.D. Thesis, Deakin University, Geelong, 2004, p. 220.